Scientific Research Publishing

Open Journal of Modern Hydrology, 2025, 15(4), 269-293
https://www.scirp.org/journal/ojmh
ISSN Online: 2163-0496
ISSN Print: 2163-0461

Seasonal and Regional Variability in Hydrological and Drought Responses in the Great Lakes Region: Impacts of SPEI Data Window Selection on Trend Detection

Katherine Clancy, Brooke Payne

College of Natural Resources, University of Wisconsin at Stevens Point, Stevens Point, USA
Email: kclancy@uwsp.edu

How to cite this paper: Clancy, K. and Payne, B. (2025) Seasonal and Regional Variability in Hydrological and Drought Responses in the Great Lakes Region: Impacts of SPEI Data Window Selection on Trend Detection. *Open Journal of Modern Hydrology*, **15**, 269-293.
https://doi.org/10.4236/ojmh.2025.154017

Received: March 21, 2025
Accepted: August 25, 2025
Published: August 28, 2025

Abstract

This study investigates seasonal and spatial variability in hydrological and drought-related responses across watersheds in the Great Lakes region, focusing on streamflow, baseflow, and the Standardized Precipitation Evapotranspiration Index (SPEI). Using daily streamflow data from 70 USGS sites (1960-2022), baseflow was separated via the HYSEP method, and watersheds were delineated using the D8 algorithm with high-resolution elevation data. Trend analyses employed Mann-Kendall and Pettitt break tests to detect temporal shifts in hydrological and climatic variables. Two SPEI datasets were compared: a full-period dataset spanning 1901-2022 and a truncated dataset aligned with the streamflow record (1960-2022). Results reveal pronounced spatial heterogeneity, with the northern region exhibiting the greatest variability and temporal dispersion in break years for baseflow and total flow. SPEI break years generally precede hydrological shifts, indicating that meteorological drought signals often emerge before hydrological responses. However, the truncated SPEI dataset shows closer temporal alignment with streamflow changes, emphasizing the critical influence of data window selection on drought interpretation. Seasonal analyses highlight stronger agreement between SPEI and hydrological trends during fall and winter, while summer shows lower correspondence, particularly in the northern region, suggesting complex interactions between climatic drivers and watershed processes. These findings underscore the importance of considering temporal alignment and regional heterogeneity when using drought indices for hydrological assessment and water resource management under changing climate conditions.

Keywords

SPEI, Drought Indices, Seasonal, Midewest, Baseflow

1. Introduction

Understanding seasonal variability in hydrological and drought-related data is essential for effective water resource management and drought mitigation, especially under the accelerating influence of climate change. Seasonal data often reveal distinct patterns that are obscured when using annual or aggregated datasets. For instance, shifts in streamflow timing in snowmelt-dominated basins have been strongly linked to increasing winter and spring temperatures, which accelerate snowmelt and alter water availability during critical warm seasons. These shifts can have profound impacts on ecosystems, agriculture, and wildfire frequency, as earlier snowmelt reduces water availability later in the year [1]-[3]. In the western United States, where up to 75% of water supplies are derived from snowmelt, trends toward earlier snowmelt-related streamflow timing have been observed, with median shifts of several days to weeks depending on elevation and region [3]. These changes are primarily driven by rising air temperatures and, to a lesser extent, precipitation variability [1] [4]. In the U.S. Midwest and other regions, seasonal streamflow patterns are influenced by climatic factors such as precipitation variability, temperature, and land use changes, with effects varying across seasons [5]. These findings underscore the importance of analyzing hydrological variables at seasonal scales to capture the complexity of drought and water availability patterns [6] [7].

The study area encompasses watersheds located across the states of Wisconsin, Michigan, which border the Great Lakes (see **Figure 1** and **Table 1**) and northern Indiana. These lakes significantly influence regional hydrology but also present

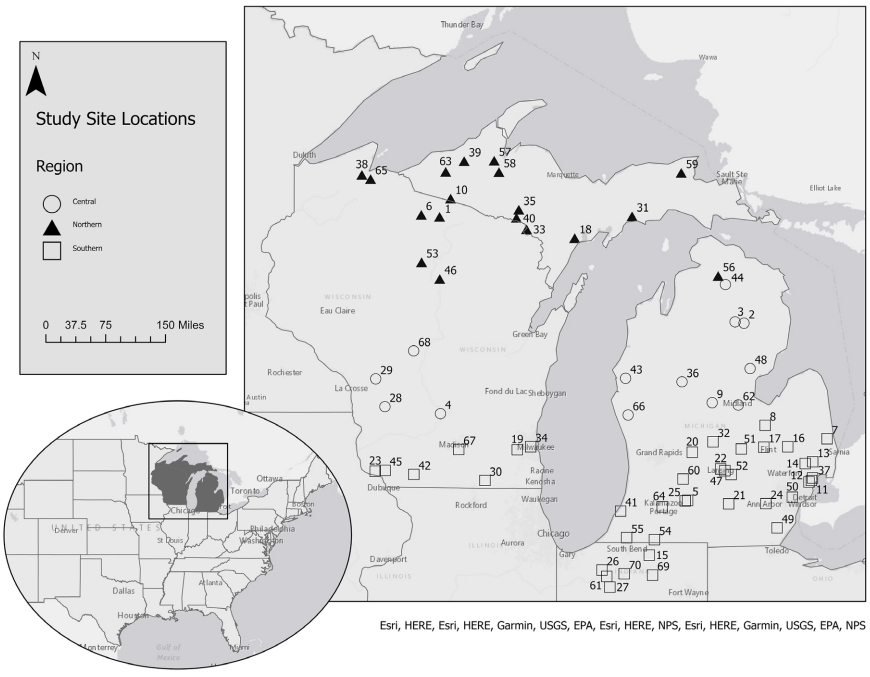

Figure 1. Location map of the study sites and their relative proximity to the Great Lakes. The numbers correspond to site information in **Table 1**.

Table 1. List of all USGS stations located including site number. Labels on Figure 1 correspond to the Map ID column.

Map ID	USGS Site No.	USGS Site Name	Region
1	05357215	Allequash Creek at County Hwy M Near Boulder Junction, WI	northern
2	04136500	Au Sable River at Mio, Mi	central
3	04136000	Au Sable River near Red Oak, Mi	central
4	05405000	Baraboo River Near Baraboo, WI	central
5	04105000	Battle Creek at Battle Creek, Mi	southern
6	05357335	Bear River Near Manitowish Waters, WI	northern
7	04159492	Black River near Jeddo, Mi	southern
8	04151500	Cass River at Frankenmuth, Mi	southern
9	04154000	Chippewa River near Mount Pleasant, Mi	central
10	04037500	Cisco Branch Ontonagon R at Cisco Lake Outlet, Mi	northern
11	04165500	Clinton River at Moravian Drive at Mt. Clemens, Mi	southern
12	04164000	Clinton River near Fraser, Mi	southern
13	04164300	East Branch Coon Creek at Armada, Mi	southern
14	04164100	East Pond Creek at Romeo, Mi	southern
15	04100500	Elkhart River at Goshen, in	southern
16	04146000	Farmers Creek near Lapeer, Mi	southern
17	04148500	Flint River near Flint, Mi	southern
18	04059500	Ford River near Hyde, Mi	northern
19	05543830	Fox River at Waukesha, WI	southern
20	04116000	Grand River at Ionia, Mi	southern
21	04109000	Grand River at Jackson, Mi	southern
22	04113000	Grand River at Lansing, Mi	southern
23	05413500	Grant River at Burton, WI	southern
24	04174500	Huron River at Ann Arbor, Mi	southern
25	04105500	Kalamazoo River near Battle Creek, Mi	southern
26	05515500	Kankakee River at Davis, in	southern
27	05517500	Kankakee River at Dunns Bridge, in	southern
28	05408000	Kickapoo River at La Farge, WI	central
29	05382325	LaCrosse River at Sparta, WI	central
30	05431486	Little Turtle Creek at Carvers Rock Road Near Clinton, WI	southern
31	04056500	Manistique River near Manistique, Mi	northern
32	04115000	Maple River at Maple Rapids, Mi	southern
33	04063522	Menominee River at Us Hwy-2 near Iron Mountain, Mi	northern
34	04087120	Menomonee River at Wauwatosa, WI	southern

Continued

35	04062500	Michigamme River near Crystal Falls, Mi	northern
36	04121500	Muskegon River at Evart, Mi	central
37	04164500	North Branch Clinton River near Mt. Clemens, Mi	southern
38	40263491	North Fish Creek Near Moquah, WI	northern
39	04040000	Ontonagon River near Rockland, Mi	northern
40	04062000	Paint River near Alpha, Mi	northern
41	04102500	Paw Paw River at Riverside, Mi	southern
42	05432500	Pecatonica River at Darlington, WI	southern
43	04122500	Pere Marquette River at Scottville, Mi	central
44	04128990	Pigeon River near Vanderbilt, Mi	central
45	05414000	Platte River near Rockville, WI	southern
46	05394500	Prairie River Near Merrill, WI	northern
47	04112500	Red Cedar River at East Lansing, Mi	southern
48	04142000	Rifle River near Sterling, Mi	central
49	04176500	River Raisin near Monroe, Mi	southern
50	04166500	River Rouge at Detroit, Mi	southern
51	04144500	Shiawassee River at Owosso, Mi	southern
52	04112000	Sloan Creek near Williamston, Mi	southern
53	05393500	Spirit River at Spirit Falls, WI	northern
54	04099000	St. Joseph River at Mottville, Mi	southern
55	04101500	St. Joseph River at Niles, Mi	southern
56	04127997	Sturgeon River at Wolverine, Mi	northern
57	04041500	Sturgeon River near Alston, Mi	northern
58	04040500	Sturgeon River near Sidnaw, Mi	northern
59	04045500	Tahquamenon River near Paradise, Mi	northern
60	04117500	Thornapple River near Hastings, Mi	southern
61	03330500	Tippecanoe River at Oswego, in	southern
62	04156000	Tittabawassee River at Midland, Mi	central
63	04036000	West Branch Ontonagon River near Bergland, Mi	northern
64	04106400	West Fork Portage Creek at Kalamazoo, Mi	southern
65	04027500	White River Near Ashland, WI	northern
66	04122200	White River near Whitehall, Mi	central
67	05429500	Yahara River at Mc Farland, WI	southern
68	05402000	Yellow River at Babcock, WI	central
69	05517000	Yellow River at Knox, in	southern
70	05516500	Yellow River at Plymouth, in	southern

challenges for hydrological and drought studies due to complex lake-groundwater

interactions, the dynamic water-land boundary, and a lack of sufficient temporal and spatial resolution in surface water gaging data. The hydrology of the Great Lakes region is further complicated by non-stationarity in long-term data sets, which hinders the detection and interpretation of trends [8]. These challenges necessitate careful site selection and data analysis to accurately assess hydrological changes and drought signals in the region.

The Great Lakes region's hydrological complexity and data limitations have been highlighted in recent studies, emphasizing the need for improved understanding of groundwater-surface water interactions and the impacts of climate variability on water resources [9] [10]. The spatial distribution of study sites across northern, central, and southern parts of Wisconsin and Michigan, as well as some sites in northern Illinois and Indiana, allows for capturing geographic variability in hydrological responses (**Figure 1**). This regional approach is critical for addressing the heterogeneity of drought impacts and streamflow variability influenced by both climatic and watershed characteristics [11] [12].

The Standardized Precipitation Evapotranspiration Index (SPEI) is a widely used drought index that integrates both precipitation and potential evapotranspiration to assess drought severity over multiple timescales. Unlike indices based solely on precipitation, SPEI accounts for the balance between water supply and atmospheric demand, making it a robust tool for evaluating the impacts of climate variability and change on hydrological systems. Its sensitivity to temperature-driven evapotranspiration allows SPEI to capture drought severity more comprehensively, which is critical for understanding water resource dynamics in the context of global warming. By incorporating atmospheric water demand, SPEI provides a more complete measure of drought conditions, making it particularly useful for evaluating meteorological drought and its potential impacts on ecosystems and water resources [13] [14].

Schnettler, S. *et al.* (2024) [8] examine the complex hydrological responses to climate variability and anthropogenic influences across Michigan and the broader Great Lakes region, focusing on the interplay between precipitation, evapotranspiration, streamflow (baseflow), and groundwater. Given the region's warming temperatures, shifting precipitation patterns, and limited groundwater data, they compared standardized annual streamflow and groundwater data with the Standardized Precipitation-Evapotranspiration Index (SPEI) to better understand water availability and drought dynamics. Baseflow, which reflects groundwater contributions to streams, was used as a proxy for groundwater where direct measurements are scarce. Their analysis revealed significant regional variability: the southern region showed increasing trends in groundwater and baseflow linked to urbanization and increased precipitation, while the northern region exhibited more complex and less synchronized hydrological responses influenced by lake-effect processes and climatic oscillations. The central region displayed mixed trends, reflecting its transitional nature between urban and natural landscapes. These findings highlight the importance of integrating multiple hydrological indicators to

capture the nuanced impacts of climate and land use on water resources.

We examined both precipitation deficits and streamflow because, although these metrics are related, they capture different aspects of drought and water availability that do not always occur simultaneously [15]. Precipitation deficits, as reflected in indices like SPEI, indicate meteorological drought by measuring the imbalance between water supply and atmospheric demand [16]-[18]. These deficits provide an early signal of potential water shortages but do not immediately translate into reduced streamflow due to watershed buffering mechanisms such as soil moisture storage, groundwater reserves, and land cover.

Streamflow, on the other hand, represents the integrated hydrological response of a watershed, reflecting actual water availability in rivers and streams. It accounts for the cumulative effects of precipitation, evapotranspiration, soil moisture, and groundwater contributions. Because of these complex interactions, streamflow reductions may lag behind precipitation deficits or be influenced by additional factors like groundwater withdrawals and land use changes that do not directly affect precipitation or SPEI [13] [14].

By analyzing both precipitation deficits and streamflow, we gain a more comprehensive understanding of drought dynamics. This dual approach allows us to capture both the onset of meteorological drought conditions and their eventual impact on hydrological systems, which is especially important in regions with complex hydrology like the Great Lakes watershed [6].

Baseflow, a component of streamflow sustained by groundwater discharge and delayed subsurface flow, responds more slowly to precipitation changes compared to total streamflow, which includes rapid surface runoff. This makes baseflow a valuable indicator of longer-term hydrological drought and groundwater availability [17]. Because baseflow integrates groundwater storage dynamics, it can reveal drought impacts not immediately apparent in precipitation or surface runoff data, highlighting different aspects of drought stress in a watershed. Seasonal analyses show that baseflow and baseflow index (BFI) exhibit significant seasonal variability and trends, with baseflow often decreasing in spring, summer, and fall, while BFI trends vary by season [18] [19].

Building on prior research that identified data limitations and regional hydrological complexities, Schnettler, S. *et al.* (2024) [8] advance understanding by systematically comparing standardized hydrological and meteorological indices over a multi-decadal period. While earlier studies emphasized the challenges of groundwater data scarcity and the need for proxies like baseflow, this study explicitly quantifies regional trends and variability, providing a more detailed spatial and temporal assessment. Furthermore, Schnettler *et al.* recognize the importance of expanding the geographic scope and incorporating seasonal data analyses to capture finer-scale hydrological dynamics. Their work sets the stage for future research to address these gaps, offering a foundation for improved drought and water resource management strategies in the Great Lakes basin under changing climate conditions [8] [20].

2. Site Location

Michigan and Wisconsin are surrounded by the Great Lakes on at least two sides, as shown in Figure 1. Despite the importance of this region, there remains a lack of sufficient knowledge regarding its hydrology and response to climatic changes. This knowledge gap is partly due to the complex nature of lake and shallow groundwater interactions, the lack of appropriate temporal and spatial resolution of gaging site data for surface water, and the lack of stationarity within long-term data sets.

Consistent with the approach used in Clancy (2023) [8] and Schnettler, S. *et al.* (2024) [8], the selection of surface water study sites for this analysis was based on several key criteria. First, sites were required to have a daily streamflow record exceeding 10 years. Second, we prioritized locations with a substantial baseflow contribution, specifically those where baseflow accounted for more than 60% of total flow. Additionally, we aimed to include a broad spectrum of watershed sizes to capture variability in hydrological responses. Lastly, we selected sites distributed across northern, central, and southern regions of the states to capture geographic variability. Due to findings in Schnettler, S. *et al.* (2024) [8], we increased the southern data set, by adding sites from in northern Indiana.

This process yielded 70 U.S. Geological Survey (USGS) sites, spanning the years 1960 to 2024, with an average baseflow contribution of 82%. Watershed sizes were grouped as follows: small watersheds ranging from 4.8×10^7 to 8.3×10^8 m^2; medium watersheds from 8.9×10^8 to 1.91×10^9 m^2; and large watersheds from 2.0×10^9 to 9.5×10^9 m^2. The locations of these watersheds are depicted in Figure 1 with USGS identifying information in Table 1, providing spatial context for the study area, while Table 1 summarizes the USGS stations, including their geographic coordinates and watershed sizes.

To categorize our surface water gaging data locations, we used latitude bands similar to those in Schnettler S. *et al.* (2024) [8]: northern locations are above 44.5˚ latitude, central locations fall between 44.3˚ and 43.5˚, and southern locations are below 43˚ latitude. This regional stratification allows for analysis of spatial variability in hydrological and drought responses across the study area. The study site stations are symbolized according to their region in Figure 1 and detailed in Table 1.

The proximity of many study sites to the Great Lakes introduces additional complexity due to lake-groundwater interactions and the dynamic water-land boundary, which can affect streamflow and baseflow patterns. These factors, combined with regional climatic variability, underscore the importance of a spatially distributed network of monitoring sites to capture the heterogeneity of hydrological responses across the region.

3. Methods

3.1. Discharge and Baseflow Data

In October 2024, we accessed the USGS National Water Information System to retrieve daily streamflow data and supporting records [21]. As described in the

site selection process, we focused on watersheds characterized by high baseflow contributions. Only sites with complete annual streamflow records from 1960 to 2022 were included in the analysis.

For baseflow separation, we applied the same methodology used in Clancy (2023) [8], which employs the HYSEP (Hydrograph Separation) program [22] [23]. All discharge data were processed using the local minimum method. Although newer techniques such as stable isotope analysis and high-resolution temperature sensing have emerged, HYSEP remains a widely accepted and practical approach for long-term flow data. A comprehensive discussion of baseflow separation methods can be found in Clancy (2023) [8]. Average baseflow and total flow values were calculated for each season for each year, along with corresponding annual averages.

3.2. SPEI

SPEI data, which are publicly available, are distributed in NetCDF format with a spatial-temporal structure consisting of raster layers that represent specific time intervals across a geographic grid [13] [24]. For Michigan and Wisconsin, the SPEI dataset spans from 1901 to 2022 with a spatial resolution of 0.5 degrees. In this study, we extracted SPEI values at a 1-month timescale for each watershed. The SPEI-1 month time scale was favored over other timescales (such as three, six, nine, and 12-month time scales) due to analysis from Clancy, 2023 [8]. This timescale was selected to assess the seasonal influence of precipitation variability on streamflow [14]. Seasonal (winter, spring, summer, fall) and annual averages were calculated from the monthly SPEI values for each year in the record. We also adjusted the SPEI data by truncating its date range to align with the corresponding discharge records for each region. This modified dataset is referred to as "SPEI Truncated Data." This adjustment was made to assess the influence of the period of record on SPEI results and to enhance comparability with the discharge data.

3.3. Watershed Delineation

The delineation of the 64 watersheds in the study area was conducted using the D8 method, a widely recognized approach available in ESRI's ArcGIS Pro Hydrology Tools. This method, as described by Troolin and Clancy (2016) [23] and originally developed by Jenson (1984) [24] [25], requires only elevation data, such as digital elevation models (DEMs) [26], and an outlet point for successful delineation. For this study, we utilized a 30-meter digital elevation model provided by the USGS [23] [24]. The resulting watershed areas and perimeters were compared with USGS-published values, and they matched within 99%, confirming the accuracy of the delineation.

3.4. Mann-Kendall Trend Test

The overall trends in baseflow, total flow, and SPEI time series data were evaluated using the Mann-Kendall tau trend test, implemented through the Kendall R package. The Mann-Kendall test is a non-parametric statistical hypothesis test that uses the rank of the data to detect trends, making it particularly useful for hydro-

logical time series analysis [27] [28]. This test has gained widespread acceptance in hydrology due to its inclusion in statistical manuals for hydrologists and its flexibility in examining the stationarity of various climate variables.

For the Mann-Kendall hypothesis test, the null hypothesis (H_0) assumes the data are random (indicating no trend), while the alternative hypothesis suggests a trend (either upward or downward). An alpha level of 0.05 was used, with p-values less than 0.05 indicating the presence of a trend. The direction of the trend was generally determined by graphical analysis. A limitation of the Mann-Kendall tau trend test is its assumption of a monotonic trend, meaning it can only detect a single trend direction. Data with multiple trends may often result in a "no trend" conclusion. For datasets exhibiting complex trends, involving both upward and downward movements, it is recommended to divide the data into subsets and analyze them separately. The main purpose of applying the Mann-Kendall test in this study was to examine and compare the trend for the total flow, baseflow, SPEI, and truncated SPEI datasets for both annual and seasonal data [8] [29].

3.5. Pettitt Break Test

To identify potential shifts in streamflow patterns over time, we applied the Pettitt Break Test, a non-parametric method used to detect a single change point in a time series. This test is particularly suited for hydrologic data, as it does not assume a specific data distribution and is effective in identifying abrupt changes in the central tendency of a dataset. The test calculates a U statistic based on the Mann-Whitney approach and determines the most likely point of change by evaluating rank-based differences before and after each candidate breakpoint. We implemented the Pettitt test in R using the pettitt.test function from the trend package. This allowed us to detect statistically significant shifts in discharge values over the period of record, providing insight into potential hydrologic regime changes. We applied this package to our seasonal datasets for baseflow, total flow, SPEI, and truncated SPEI, as well as to the corresponding annual data [30] [31].

4. Results

4.1. Baseflow and Total Flow Breaks

The analysis of Pettitt break years across USGS stations reveals a broad temporal range of hydrological changes for the annual data with the earliest detected breaks occurring in 1929 and the most recent in 2015 for both baseflow and total flow. Overall, the mean break year for baseflow is approximately 1977.7 (standard deviation 18.9 years), while for total flow it is slightly later at 1979.7 (standard deviation 18.5 years), indicating considerable variability in the timing of significant hydrological shifts across the dataset.

When stratified by region, both datasets show the northern region as the most temporally diverse and variable (**Figure 2** and **Figure 3**). For baseflow, break years in the northern region span from 1929 to 2015, with a higher mean of 1985.6 and a larger standard deviation of 22.8 years. Similarly, total flow break years in the

northern region range from 1929 to 2013, with the highest mean of 1985.5 and the greatest variability (standard deviation 21.5 years) of the regions. This suggests that hydrological changes in the northern region are more pronounced and temporally dispersed compared to other regions.

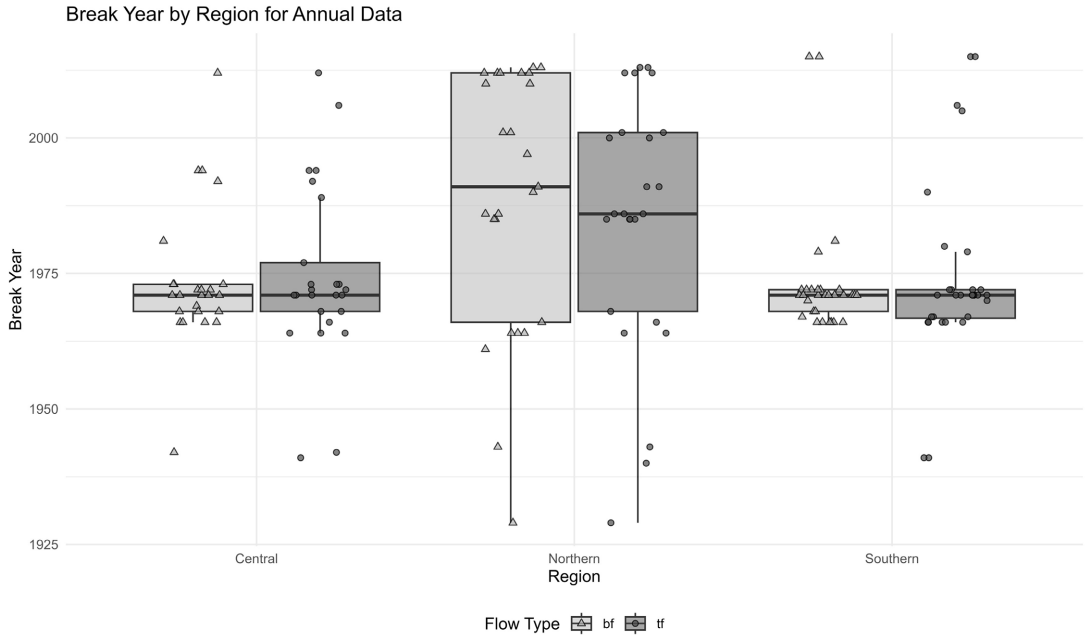

Figure 2. The Pettitt break year for total flow (tf) and baseflow (bf) from 70 USGS gaging stations by regions. The break year for the annual average of the discharge is very similar to the baseflow break year.

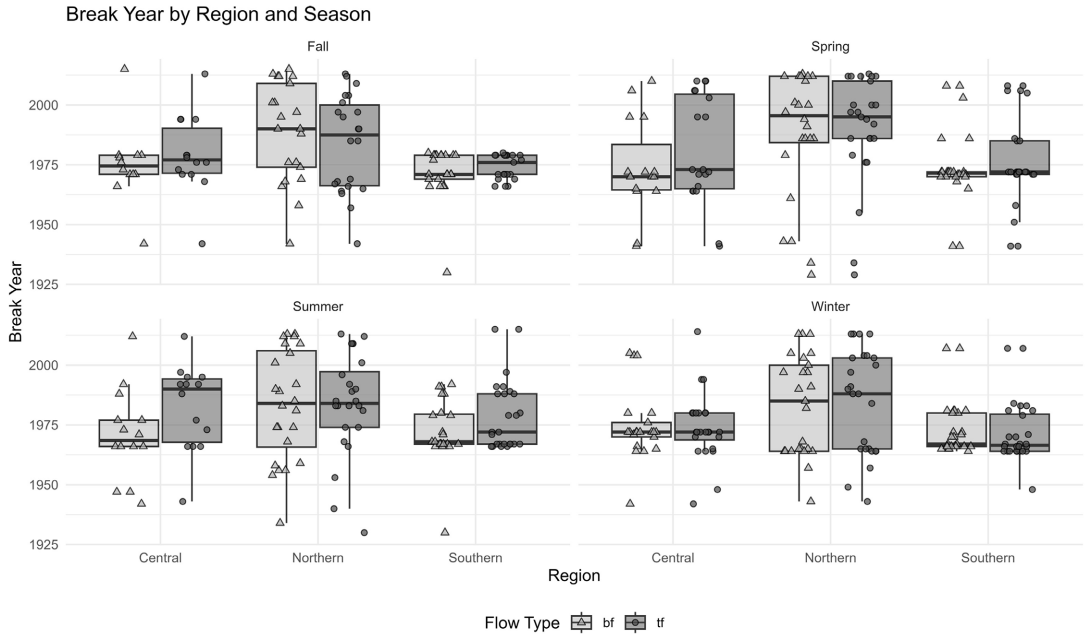

Figure 3. The Pettitt break year for total flow (tf) and baseflow (bf) from 70 USGS gaging stations by regions and seasons. Note that the test indicates some differences in the southern region in spring and the central regions in summer.

As shown in Figure 2, the central region exhibits a narrower range of break years for both baseflow (1941 to 2015, mean 1973.6, standard deviation 17.0) and total flow (1941 to 2014, mean 1978.5). The southern region shows the least temporal dispersion, with baseflow break years ranging from 1930 to 2008 (mean 1972.8, standard deviation 12.7) and total flow break years from 1941 to 2015 (mean 1975.2, standard deviation 13.9), possibly indicating relatively more stable hydrological patterns in this region.

Seasonal analyses further highlight variability in break years as shown in Figure 3, For baseflow, fall break years range from 1930 to 2015 (mean 1978.9), spring from 1929 to 2013 (mean 1979.0), summer from 1930 to 2013 (mean 1976.3), and winter from 1942 to 2013 (mean 1976.9). Total flow, shown in Figure 3 shows similar seasonal patterns, with spring and summer exhibiting wider ranges and higher variability, especially in the northern region, compared to fall and winter.

Specific stations with notable breaks shown in Figure 3 reveals distinct regional and seasonal patterns for baseflow. In the central region, stations such as Au Sable River near Red Oak, MI (2004, winter) and Cass River at Frankenmuth, MI (1941, spring) stand out for baseflow, while the same Cass River station aligns closely with total flow trends. The northern region features stations with multiple and temporally dispersed break years, such as La Crosse River at Sparta, WI, which experienced multiple baseflow breaks across all seasons (2015, 2010, 2012, 2005). The southern region includes stations like West Fork Portage Creek at Kalamazoo, MI, showing break years in both baseflow (2007, 2008) and total flow (summer and winter seasons), highlighting some consistency across flow types. Notable outlier stations include the Sturgeon River near Sidnaw, MI (northern region, fall season), which shows early break years in both datasets, and the West Fork Portage Creek at Kalamazoo, MI (southern region), with break years significantly earlier or later than regional averages in both baseflow and total flow. Conversely, stations such as the Grand River at Lansing, MI (southern region, spring) exhibit break years closely aligned with regional trends in total flow. Station locations are shown in Figure 1 cross referenced with data from Table 1.

As Figure 2 and Figure 3 show that overall, the northern region demonstrates the greatest diversity and number of outliers in break years for both baseflow and total flow, as evidenced by its wider range, higher standard deviations, and multiple stations with temporally dispersed breaks. This suggests that hydrological changes in both baseflow and total flow timing are more variable and pronounced in the northern region compared to the central and southern regions, which show more stable and consistent patterns.

4.2. SPEI Pettitt Break Years

The SPEI and SPEI Truncated break years are shown in comparison to the total flow and baseflow in Figure 4 and Figure 5, respectively. Overall, the SPEI break year ranges from 1931 to 2012, with an average break year around 1969.8. The data shows a moderate level of variability, with a standard deviation of approximately 20.7 years, indicating that the timing of the break year varies considerably

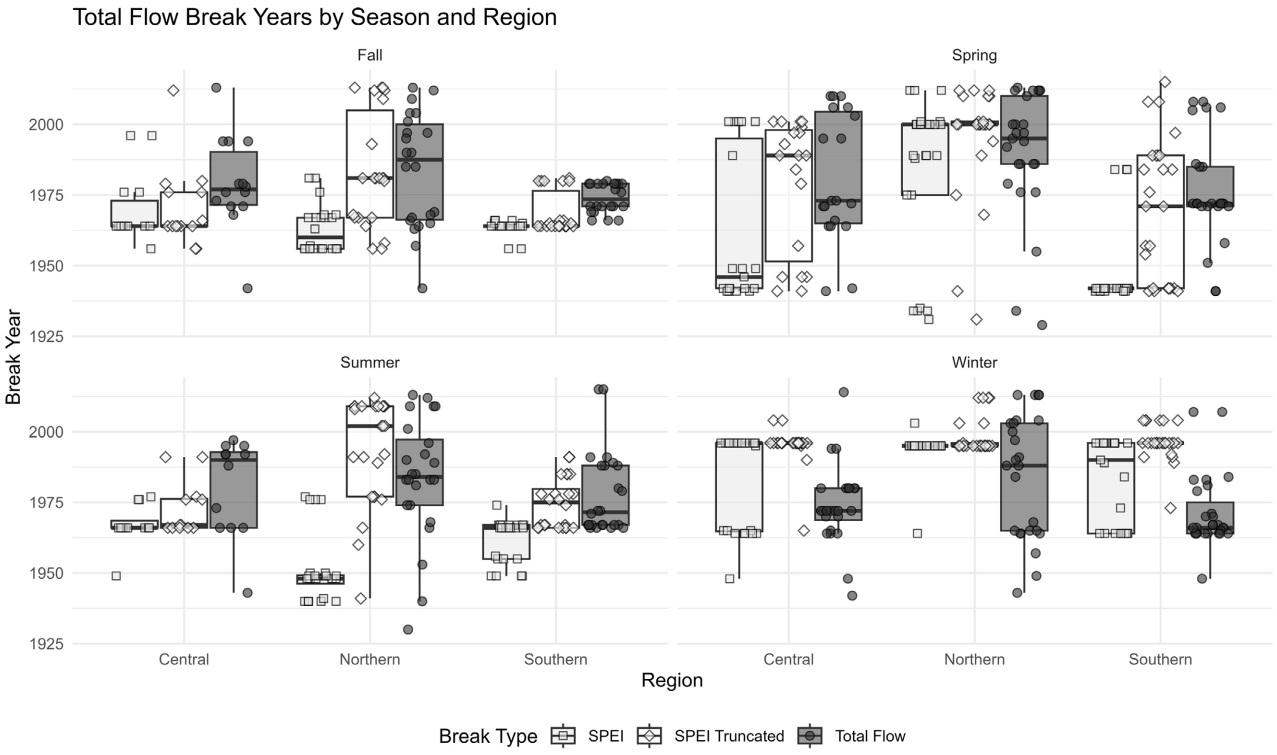

Figure 4. The Pettitt break year for SPEI, SPEI truncated, and Total Flow from 70 USGS gaging stations by regions and seasons. SPEI truncated refers to SPEI data that has start and end dates matching the closest gaging station. Note that the test indicate that SPEI truncated is closer to the total flow values for fall, spring, and summer break year for the northern region.

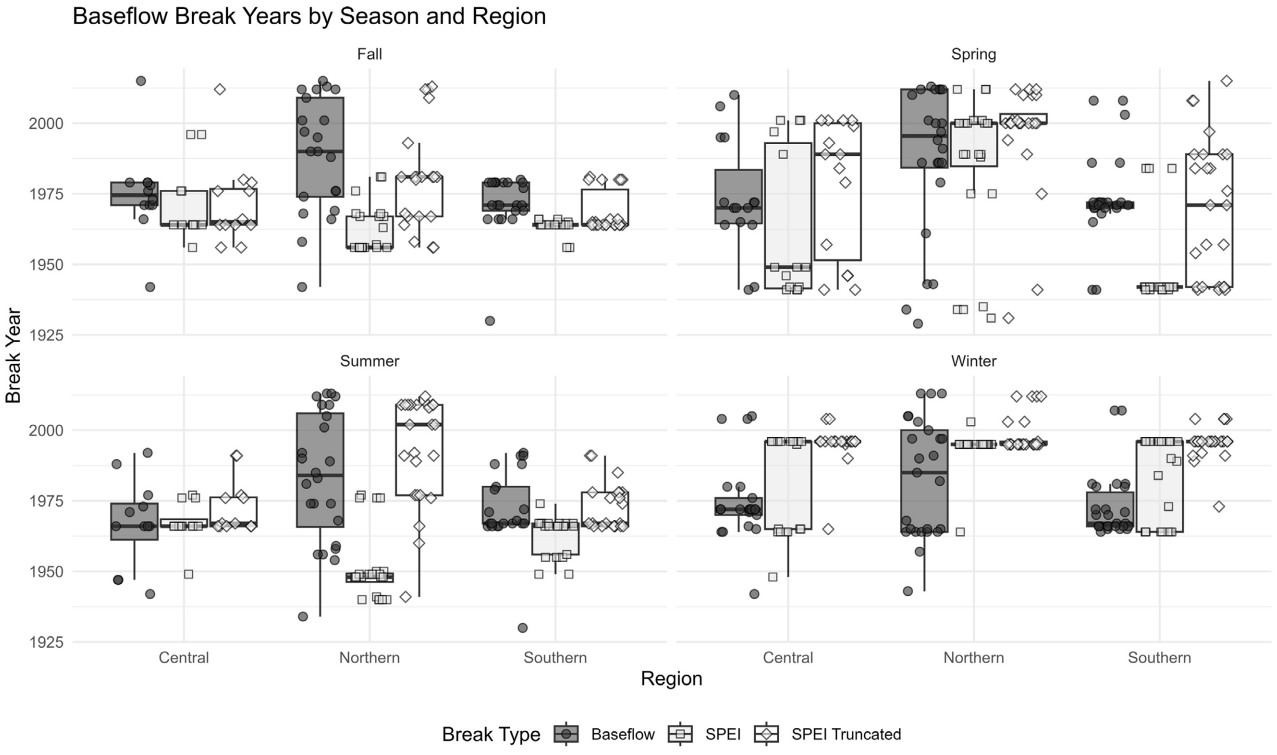

Figure 5. The Pettitt break year for SPEI, SPEI truncated, and Baseflow from 70 USGS gaging stations by regions and seasons. SPEI truncated refers to SPEI data that has start and end dates matching the closest gaging station.

across the dataset. Notably, the earliest break year of 1931 appears in the dataset, highlighting some early occurrences of the break. Some stations with unusually early break years include Basswood River near Winton, MN (1934), Bear River near Manitowish Waters, WI (1935), Little Fork River at Littlefork, MN (1931), and North Fish Creek near Moquah, WI (1934). On the other hand, stations such as Au Sable River at Mio, MI (2012), Chippewa River near Mount Pleasant, MI (2012), Pigeon River near Vanderbilt, MI (2012), and Tahquamenon River near Paradise, MI (2012) have notably late break years. SPEI values come from the geographic coordinates as the USGS stations that are shown in Figure 1 cross referenced with data from Table 1.

When examining the data by region, the northern region exhibits the widest range of break years, spanning from 1931 to 2012, and also has the highest variability with a standard deviation of about 23.2 years. This indicates more variability in SPEI Break year in the northern region compared to others. Early outlier stations in the northern region include Basswood River near Winton, MN (1934), Bear River near Manitowish Waters, WI (1935), Little Fork River at Littlefork, MN (1931), and North Fish Creek near Moquah, WI (1934). Late outliers include Ford River near Hyde, MI (2012), Manistique River near Manistique, MI (2012), and Tahquamenon River near Paradise, MI (2012). The central region follows closely with break years ranging from 1941 to 2001 and a standard deviation of roughly 19.8 years, with early outliers such as Tittabawassee River at Midland, MI (1941) and Pere Marquette River at Scottville, MI (1942). The southern region shows a narrower range from 1941 to 1996 and the least variability, with a standard deviation of approximately 17.4 years. Late outliers in the southern region include Battle Creek at Battle Creek, MI (1996) and Kalamazoo River near Battle Creek, MI (1996).

Looking at the data by season, the spring season shows the greatest variability and range, with break years extending from 1931 to 2012 and a standard deviation of nearly 27.8 years. This wide range and high standard deviation indicate more variability in SPEI Break year during spring. Late outliers in spring include Ford River near Hyde, MI (2012), Manistique River near Manistique, MI (2012), and Tahquamenon River near Paradise, MI (2012). Summer and winter seasons have more moderate ranges and variability, with summer ranging from 1940 to 1977 and winter from 1948 to 2003. Early outliers in summer include Bear River near Manitowish Waters, WI (1940) and Little Fork River at Littlefork, MN (1941). The fall season stands out as the most consistent, with break years confined between 1956 and 1996 and the lowest standard deviation of about 8.5 years, indicating more consistency in break years during fall. Late outliers in fall include Kickapoo River at La Farge, WI (1996) and La Crosse River at Sparta, WI (1996). Additionally, winter has the highest average break year at around 1987, suggesting that break years tend to occur later in the year during this season.

Overall, the SPEI Truncated year ranges from 1931 to 2015, with an average SPEI Truncated year around 1984.2. The data shows moderate variability, with a standard deviation of approximately 19.0 years. Some stations with unusually

early SPEI Truncated years include Little Fork River at Littlefork, MN (1931), Prairie River near Merrill, WI (1941), and Cass River at Frankenmuth, MI (1941). Stations with notably late SPEI Truncated y years include Bear River near Manitowish Waters, WI (2013), North Fish Creek near Moquah, WI (2013), and Elkhart River at Goshen, IN (2015).

By region, the northern region has the widest range of SPEI Truncated years, from 1931 to 2013, with the highest variability (std dev ~17.9). Early outliers in the northern region include Little Fork River at Littlefork, MN (1931) and Bear River near Manitowish Waters, WI (1941). Late outliers include Bear River near Manitowish Waters, WI (2013) and North Fish Creek near Moquah, WI (2013). The central region ranges from 1941 to 2012, with early outliers such as Cass River at Frankenmuth, MI (1941) and Clinton River at Mt. Clemens, MI (1942). The southern region ranges from 1941 to 2015, with late outliers like Elkhart River at Goshen, IN (2015).

By season, spring shows the greatest variability and range, from 1931 to 2015, with early outliers including Little Fork River at Littlefork, MN (1931) and Prairie River near Merrill, WI (1941). Summer and fall have moderate ranges, with fall ranging from 1956 to 2013 and summer from 1941 to 2012. Winter has the narrowest range, from 1965 to 2012, and the lowest variability (std dev ~6.6). Late outliers in fall include stations like Kickapoo River at La Farge, WI (2013), while summer and winter have fewer extreme outliers.

Overall, the comparison between SPEI-derived break and SPEI Truncated y years and baseflow data reveals notable temporal variability. Baseflow years span from the late 1920s to the early 2010s, with an average around the mid-1970s to mid-1980s depending on region and season. Generally, SPEI break year tends to precede the baseflow year, indicating that climatic drought signals often emerge before hydrological responses are observed. Conversely, SPEI Truncated year, which aligns SPEI data to USGS station years, tends to lag behind baseflow year, reflecting a temporal adjustment to hydrological timing. Outlier stations such as Little Fork River at Littlefork, MN (SPEI break year 1931) and Bear River near Manitowish Waters, WI (SPEI Truncated year 2013) exemplify the wide range of timing differences observed in the dataset.

Regionally, the northern region exhibits the greatest temporal offset, with SPEI break year leading baseflow year by nearly 12 years on average, and SPEI Truncated year lagging by about 7 years. Early outliers in this region include Little Fork River at Littlefork, MN (1931) and Bear River near Manitowish Waters, WI (1935), while late outliers such as Ford River near Hyde, MI (2012) and Tahquamenon River near Paradise, MI (2012) highlight the extended range of hydrological responses. The central region shows a smaller lead time of less than one year for SPEI break year relative to baseflow, with SPEI Truncated year occurring approximately 8.6 years later. Notable early outliers here include Tittabawassee River at Midland, MI (1941) and Pere Marquette River at Scottville, MI (1942). The southern region demonstrates a moderate lead time of nearly 8 years for SPEI break year and a lag of about 4.8 years for SPEI Truncated year, with late outliers such as Battle Creek at Battle Creek, MI (1996) and Kalamazoo River near Battle Creek, MI (1996).

Seasonally, the temporal relationships vary markedly. During fall, spring, and summer, SPEI break year consistently precedes baseflow year by approximately 14 to 17 years, suggesting early climatic signals before hydrological changes. For example, Kickapoo River at La Farge, WI (fall, 1996) and Little Fork River at Littlefork, MN (summer, 1941) represent outliers with early or late break years. In contrast, winter shows a reversal, with SPEI break year lagging baseflow year by over 10 years on average. SPEI Truncated year follows a similar pattern, with minimal lag in fall but increasing lag through spring and summer, peaking in winter with a lag of nearly 20 years. This seasonal variability highlights the complex interplay between climatic drought indicators and hydrological responses, emphasizing the need for seasonally nuanced interpretations.

4.3. Mann-Kendall Trend Test

4.3.1. Discharge (Total Flow and Baseflow Trends)

As shown in Figure 6, both baseflow and total annual flow data show a predominance of "Up" trends in the southern region, with baseflow having 68 "Up" trends

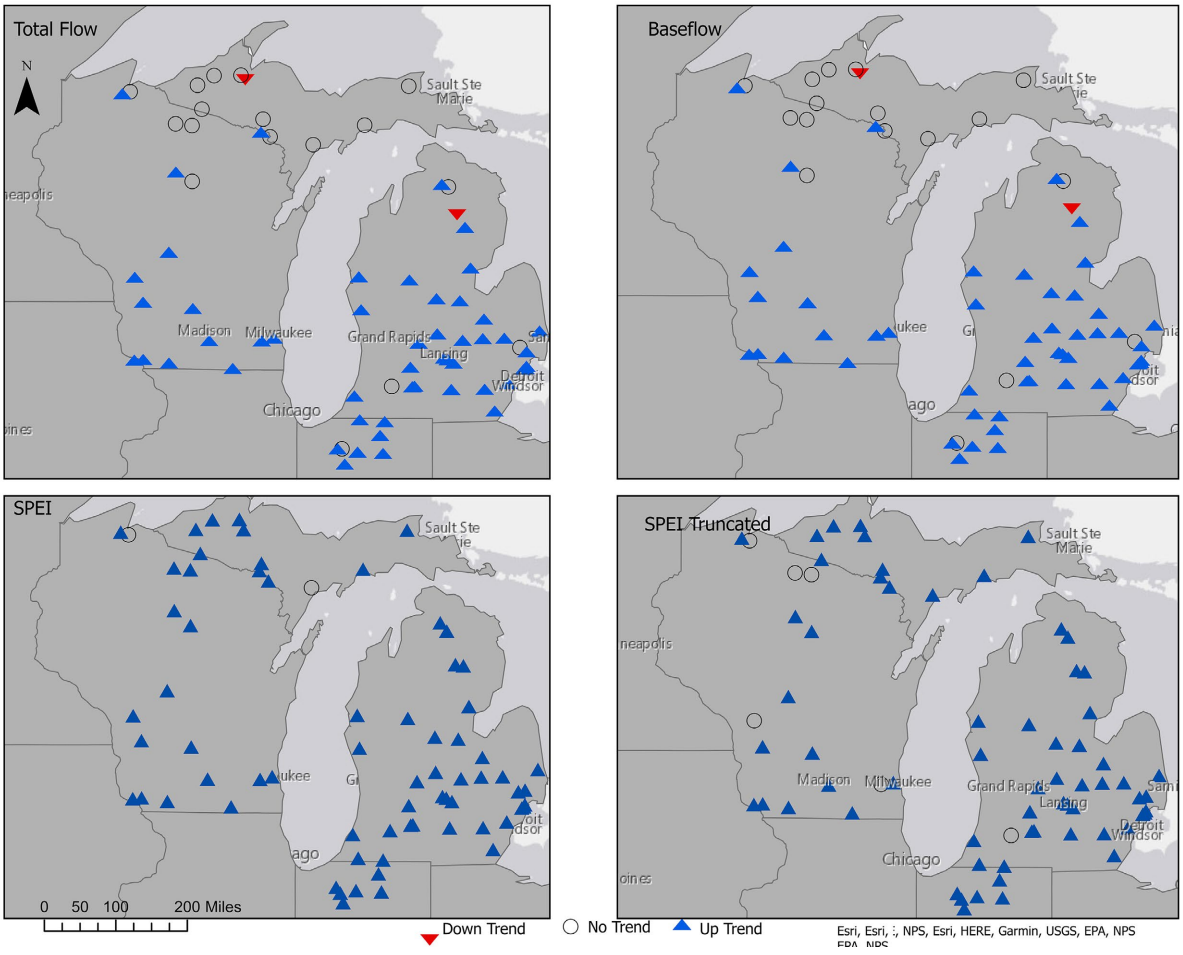

Figure 6. Mann-Kendall trend results for annual average discharge, annual average baseflow, and annual-averaged SPEI (1-month). The SPEI is calculated over the full available record (1902-2024). The "SPEI Truncated" dataset is based on the same 1-month SPEI but constrained to the time period that matches the discharge record for each station.

and total flow 68. The central region also shows more "Up" trends for baseflow (69) compared to total flow (69), while the northern region has a higher count of "Not Significant" trends for both baseflow (12) and total flow (12). However, total flow exhibits more "Down" trends in the central (0) and northern (2) regions compared to baseflow (0 and 2, respectively). This suggests that while baseflow and total flow often agree on upward trends, total flow tends to show more downward trends, especially in the central and northern regions.

Seasonal data are shown in Figure 7 (fall), Figure 8 (spring), Figure 9 (summer) and Figure 10 (winter). Both baseflow and total flow show the highest number of "Up" trends in winter, with baseflow at 47 and total flow at 14. fall also shows a strong "Up" trend for both, with baseflow at 39 and total flow at 47. However, baseflow has more "Up" trends in winter and summer compared to total flow, which shows a more balanced distribution of "Up" trends across fall, summer, and winter. Notably, total flow has more "Down" trends in winter (8) and summer (8) than baseflow (6 and 8, respectively), indicating some seasonal disagreement in downward trends.

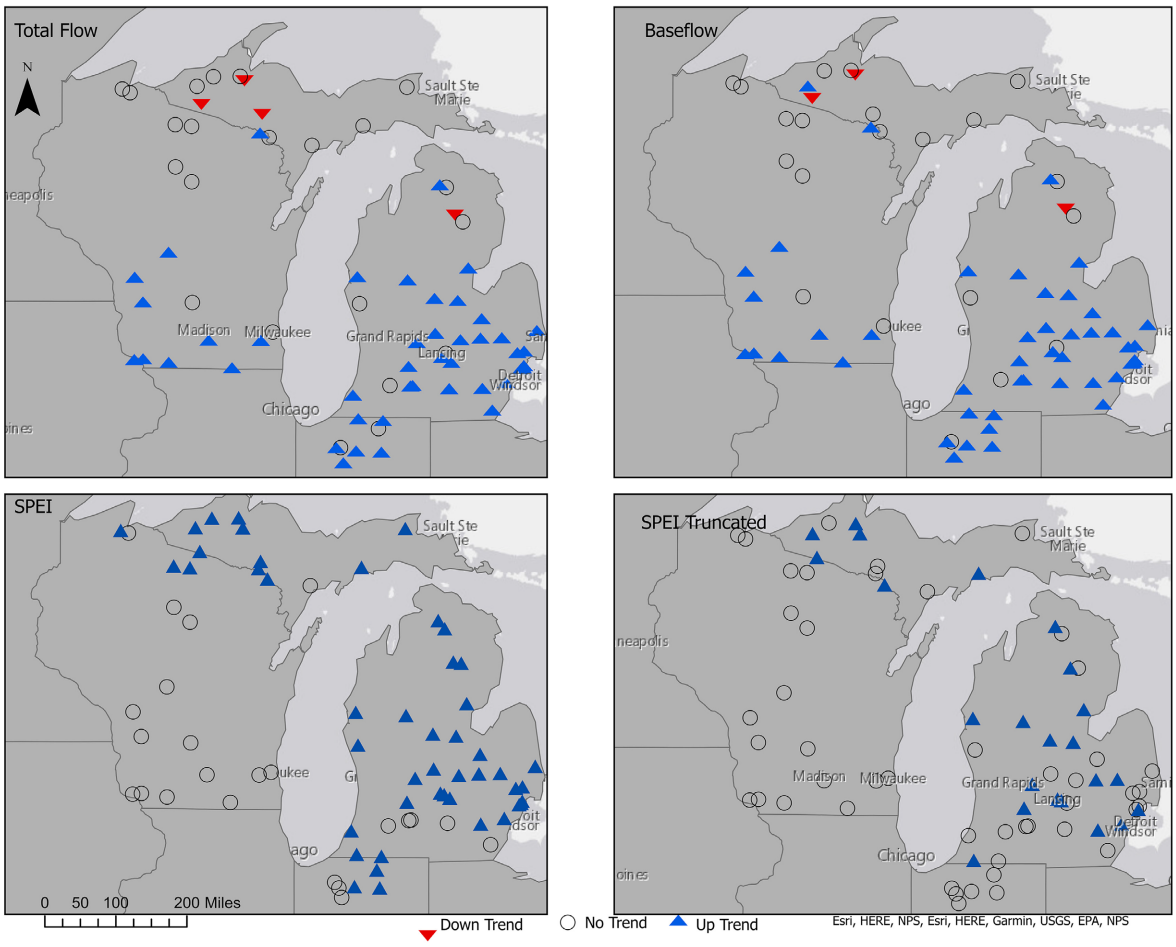

Figure 7. Mann-Kendall trend results for fall average discharge, fall average baseflow, and fall-averaged SPEI (1-month). The SPEI is calculated using the full available period (1902-2024). The "SPEI Truncated" dataset uses the same 1-month SPEI but is limited to the time period that matches the discharge record for each station.

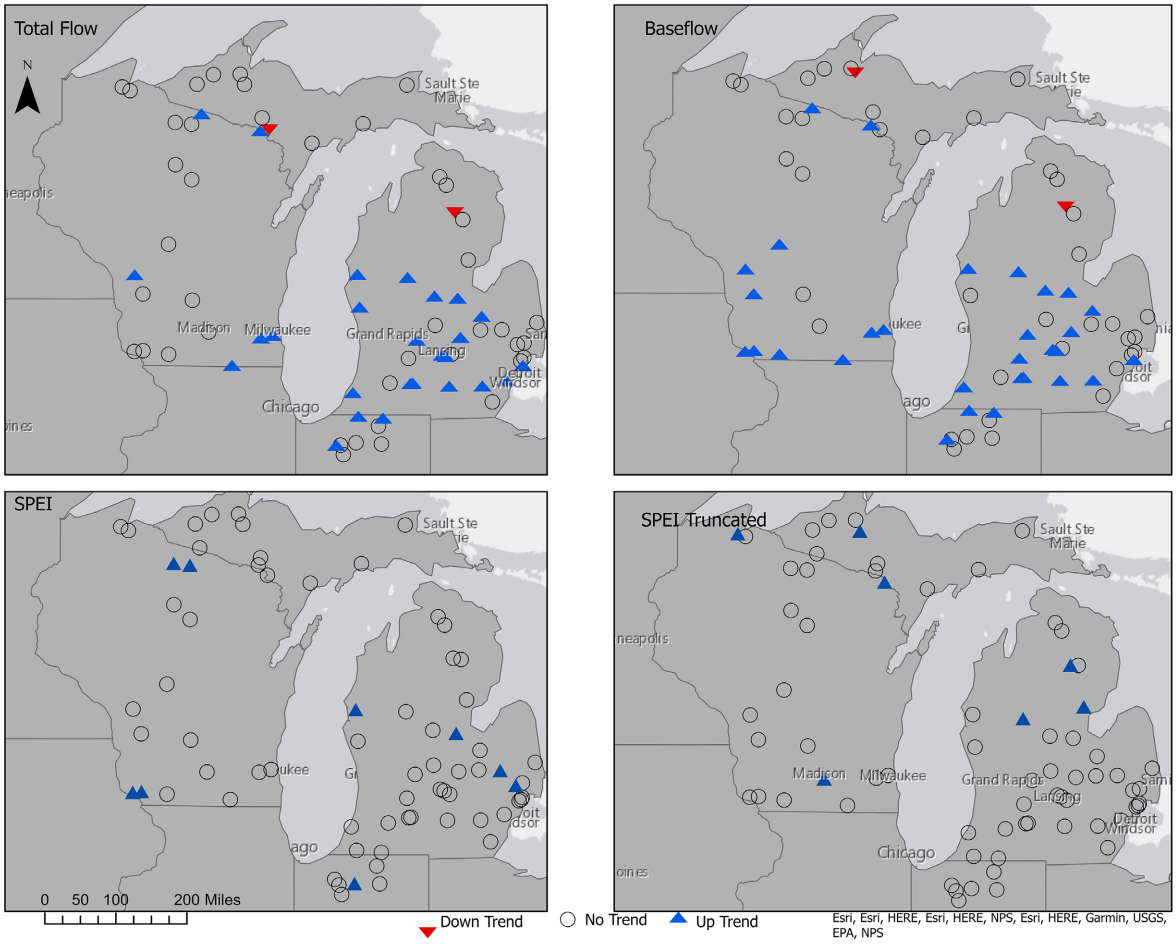

Figure 8. Mann-Kendall trend results for spring average discharge, spring average baseflow, and spring-averaged SPEI (1-month). The SPEI is calculated using the full available period (1902-2024). The "SPEI Truncated" dataset uses the same 1-month SPEI but is limited to the time period that matches the discharge record for each station.

Overall, baseflow tends to have a higher number of "Up" trends and fewer "Down" trends compared to total flow, which shows a greater presence of "Not Significant" and "Down" trends. This pattern suggests that baseflow may be more stable or consistently increasing, while total flow is more variable.

In summary, baseflow and total flow trends often align and show upward trends, particularly in the southern region and during winter and fall seasons. However, total flow tends to reveal more downward and non-significant trends, especially in the central and northern regions and during summer and winter, highlighting differences in how these two flow components respond to environmental factors.

4.3.2. SPEI (Entire Record)

In this study, SPEI trend counts reveal that the southern region generally exhibits higher numbers of "up" trends, with 68 occurrences in fall and 8 in spring, while the northern and central regions show more mixed distributions, such as mostly "up" trends in northern fall and in central fall.

Seasonal data are shown in Figure 7 (fall), Figure 8 (spring), Figure 9 (summer)

and Figure 10 (winter) and compared to flow data (baseflow and total flow). SPEI trends analyzed across different regions and seasons highlight distinct temporal and spatial variability of climatic moisture conditions. The southern region shows a predominance of "up" trends, particularly during fall and summer, with 49 and 69occurrences respectively, indicating increasing moisture availability or reduced drought severity. Conversely, the northern and central regions display a more-balanced distribution between "no trend" and "up" categories, such as 64 "no trend" and 8 "up" in northern spring, and 2 "no trend" and 70 "up" in central spring, reflecting greater climatic variability or stability in moisture conditions. Seasonal differences are also pronounced, with spring generally showing higher counts of "no trend" (e.g., 64 in southern spring), suggesting relatively stable moisture conditions, while summer and winter tend to have more "up" trends, such as 70 and 53 in northern summer and winter respectively, indicative of wetter conditions or recovery from drought.

When comparing SPEI trends with hydrological responses, specifically baseflow and total flow trends, the analysis reveals varying degrees of agreement

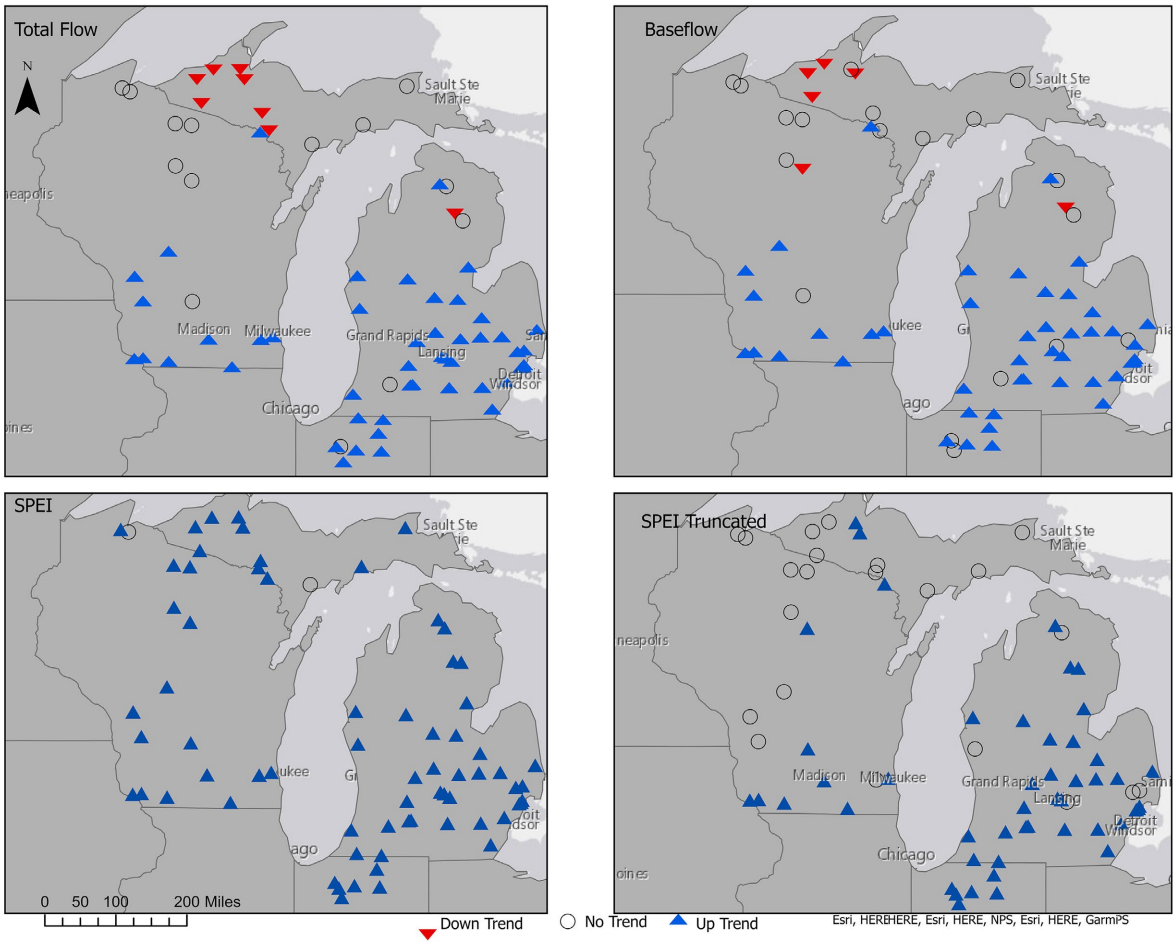

Figure 9. Mann-Kendall trend results for summer average discharge, summer average baseflow, and summer -averaged SPEI (1-month). The SPEI is calculated using the full available period (1902-2024). The "SPEI Truncated" dataset uses the same 1-month SPEI but is limited to the time period that matches the discharge record for each station.

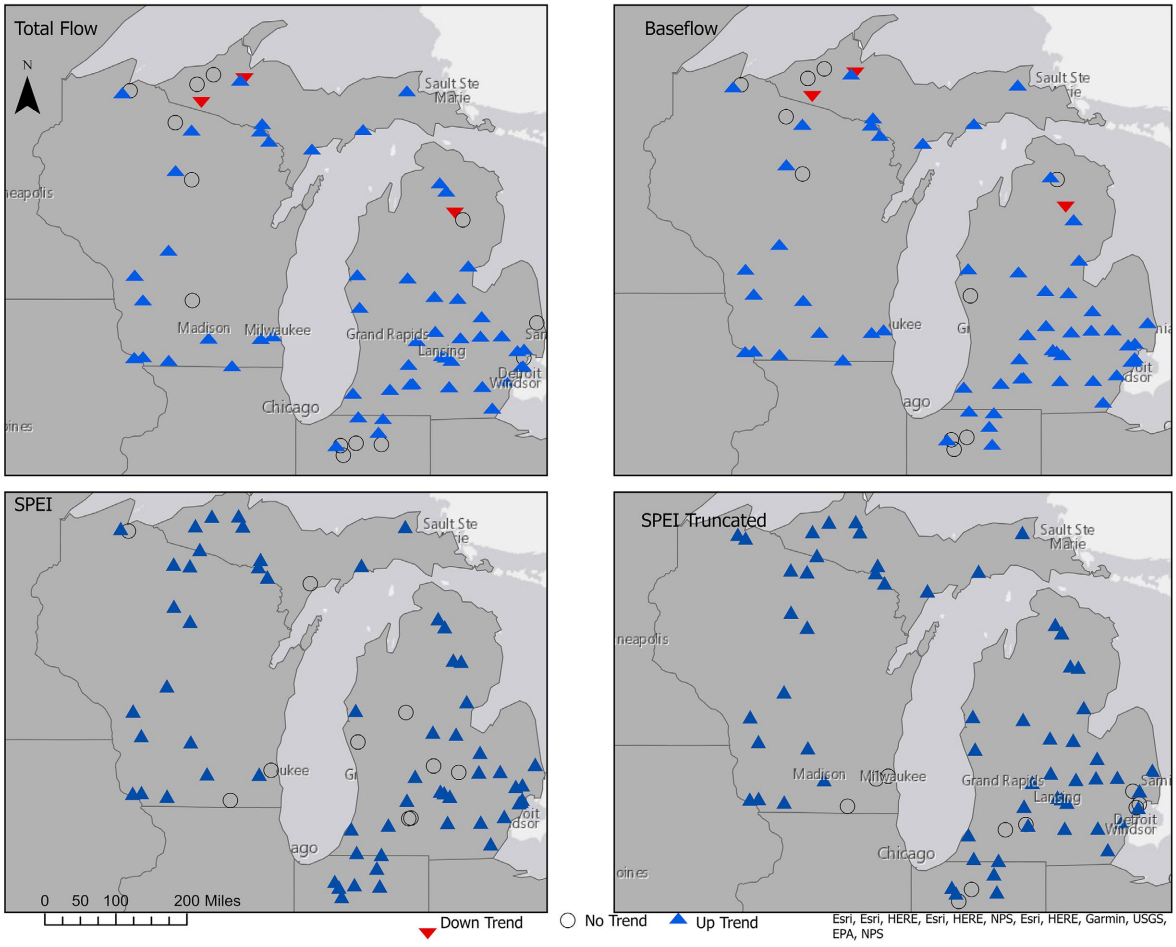

Figure 10. Mann-Kendall trend results for winter average discharge, winter average baseflow, and winter -averaged SPEI (1-month). The SPEI is calculated using the full available period (1902-2024). The "SPEI Truncated" dataset uses the same 1-month SPEI but is limited to the time period that matches the discharge record for each station.

dependent on region and season. Both baseflow and total flow align most closely with SPEI in the southern region during summer and winter, where baseflow agreement rates reach 82.2% and 81.1%, and total flow agreement rates peak at 95.6% and 73.6%, respectively. Baseflow shows higher agreement than total flow in central winter (77.8% vs. 62.2%) and northern fall (37.2% vs. 32.6%), suggesting a stronger correspondence with SPEI in these contexts. Conversely, total flow exhibits markedly higher agreement in southern summer (95.6%) compared to baseflow (82.2%). The northern summer season presents the lowest agreement rates for both baseflow and total flow at 25.0%, highlighting a period of divergence between hydrological responses and climatic trends. These findings underscore the complex interplay between climatic indices and hydrological components, emphasizing the importance of considering both regional and seasonal variability when interpreting flow responses to climatic drivers.

4.3.3. SPEI (Truncated Record)

The truncated Standardized Precipitation-Evapotranspiration Index (SPEI) trend

analysis, which aligns the climatic data period with the station flow data (covering the same years as the flow records), reveals nuanced regional and seasonal patterns in moisture availability. The truncated SPEI trends show a higher prevalence of "no trend" categories in the northern and southern regions, with 3 and 2 occurrences respectively, compared to 1 in the central region. Seasonal data are shown in Figure 7 (fall), Figure 8 (spring), Figure 9 (summer) and Figure 10 (winter) and compared to flow data (baseflow and total flow) and SPEI data. Conversely, the "up" trend counts are relatively balanced across regions, with 71 in central, 69 in northern, and 70 in southern. Seasonally, the truncated SPEI data indicate a dominance of "no trend" during spring (56 occurrences) and fall (43 occurrences), while summer and winter exhibit more "up" trends, with 21 and 62 occurrences respectively. This distribution suggests that moisture conditions during spring and fall are relatively stable, whereas summer and winter experience more pronounced increases in moisture availability or reduced drought severity. When examining the agreement between the truncated SPEI trends and hydrological responses, baseflow and total flow trends show varying correspondence across regions and seasons. Baseflow agreement rates with truncated SPEI range from 32.4% in central spring to a high of 82.2% in central winter. Northern regions generally exhibit moderate to high agreement, peaking at 71.4% in spring and maintaining above 58% in other seasons. Southern regions show lower agreement in fall (31.8%) and spring (48.0%) but higher correspondence in summer (77.8%) and winter (73.6%). Total flow agreement rates follow a similar pattern, with slightly lower agreement in central spring (38.2%) compared to baseflow, and the highest agreement in southern summer (82.2%). These results highlight that hydrological responses to climatic moisture changes, as captured by the truncated SPEI, are seasonally and regionally variable, with stronger alignment during wetter periods and in certain regions.

In comparison, the full-period SPEI data, which spans a longer timeframe from 1902 to 2024, shows generally higher agreement rates between SPEI and flow trends. For example, in the southern region during summer and winter, total flow agreement rates reached 95.6% and 73.6%, respectively, compared to 82.2% and 73.6% in the truncated SPEI analysis. Baseflow agreement in central winter was also high in both datasets (77.8% in full SPEI and 82.2% in truncated SPEI). The full SPEI data tends to show fewer "no trend" cases, reflecting its broader temporal coverage and capturing more climatic variability. Both datasets consistently identify northern summer as a period of low agreement between climatic and hydrological trends, underscoring the complexity of hydrological responses in this region and season. Overall, while the truncated SPEI provides a temporally aligned perspective with the flow data, the full SPEI captures broader climatic variability, and both are valuable for understanding the interplay between climate and hydrology across spatial and temporal scales.

5. Discussion

This study reveals significant temporal and spatial variability in hydrological and

drought-related responses across the northern, central, and southern regions, with pronounced anomalies particularly evident in the northern region. The broad range of break years for baseflow and total flow in the northern region—from as early as 1929 to as recent as 2015 for baseflow and 2013 for total flow—along with the highest standard deviations (22.8 years for baseflow and 21.5 years for total flow), indicate a highly variable and temporally dispersed pattern of hydrological change (**Figure 6**). This contrasts with the central and southern regions, which show narrower break year ranges and lower variability (e.g., southern baseflow break years range from 1930 to 2008 with a standard deviation of 12.7 years). Such variability in the northern region likely reflects complex watershed processes, including snowmelt timing shifts, groundwater interactions, and heterogeneous land use impacts [3] [20].

Seasonally, the northern region's spring and summer break years exhibit wider ranges and higher variability compared to fall and winter, with spring baseflow break years spanning 1929 to 2013 (mean 1979.0) and summer from 1930 to 2013 (mean, 1976.3). This seasonal variability aligns with the sensitivity of snowmelt-driven hydrology to warming temperatures during these months, which can accelerate snowmelt and alter streamflow timing, leading to earlier peak flows and reduced late-season water availability [1] [2]. The multiple break years observed at stations like La Crosse River at Sparta, WI, which experienced baseflow breaks in 2005, 2010, 2012, and 2015 across all seasons, further illustrate episodic hydrological regime shifts rather than uniform trends (**Figure 7**).

The SPEI break year analysis complements these findings, with the northern region showing the widest range of break years (1931 to 2012) and the highest variability (standard deviation ~23.2 years). Early break year outliers such as Little Fork River at Littlefork, MN (1931) and Bear River near Manitowish Waters, WI (1935) contrast with late break years like Tahquamenon River near Paradise, MI (2012), highlighting spatial heterogeneity in climatic drought onset. Notably, the spring season exhibits the greatest variability in SPEI break years (1931 to 2012, with a standard deviation of 27.8 years), reinforcing the idea that climatic drought signals during this season are highly variable and may precede hydrological responses by significant intervals (**Figure 8**).

A key finding is the temporal offset between SPEI and hydrological break years, particularly in the northern region, where SPEI break years lead baseflow break years by nearly 12 years on average. This suggests that meteorological drought conditions, as captured by SPEI, often manifest well before hydrological drought indicators such as baseflow changes, likely due to watershed storage and groundwater buffering delaying hydrological responses [15] [17]. Conversely, the truncated SPEI break years, which align the climatic data period with hydrological records, show closer correspondence with baseflow and total flow break years, especially in fall, spring, and summer for the northern region (**Figure 8** and **Figure 9**). This indicates that truncated SPEI break years provide a better temporal match for discharge data, suggesting that the timing of hydrological break years might

be predicted or indicated by what SPEI reveals when the data periods are synchronized (**Figure 9**).

In contrast, the southern region shows more stable hydrological patterns, with narrower break year ranges and lower variability (e.g., baseflow break years from 1930 to 2008, std dev 12.7 years). This region also exhibits a predominance of upward trends in both baseflow and total flow, particularly during winter and fall, with baseflow showing 70 "Up" trends and total flow 70 in the southern region overall. These upward trends correspond with SPEI results indicating increased moisture availability or reduced drought severity, especially in fall (72 "Up" trends) and summer (70 "Up" trends). The high agreement rates between SPEI and flow trends in the southern region—up to 95.6% for total flow in summer and 81.1% for total flow in winter—suggest a more direct coupling between climatic moisture conditions and hydrological responses here [13] [14].

Seasonal discrepancies in trend agreement are evident, particularly in the northern summer, where agreement between SPEI and both baseflow and total flow trends drops to 25%. This low correspondence indicates that factors beyond climatic moisture availability, such as groundwater withdrawals, land use changes, or complex watershed storage, may decouple hydrological responses from meteorological drought signals during this season [18]. The reversal of temporal relationships in winter, where SPEI break year lags baseflow break years by over 10 years on average, likely reflects snow accumulation and melt processes that delay hydrological drought manifestations relative to climatic drought indicators [3].

The truncated SPEI analysis, which aligns climatic data with the temporal window of hydrological records, reveals a higher prevalence of "no trend" categories in spring and fall, suggesting relative stability in moisture conditions during these seasons. However, summer and winter show more "up" trends, consistent with wetter conditions or drought recovery phases. Agreement rates between truncated SPEI and hydrological trends vary regionally and seasonally, with central winter showing high baseflow agreement (82.2%) and northern spring maintaining above 70% agreement, highlighting the importance of seasonal context in interpreting drought-hydrology relationships (**Figures 1-5**).

Overall, the findings emphasize the critical role of seasonality, regional heterogeneity, and temporal data coverage in understanding drought and hydrological dynamics. The pronounced anomalies and temporal offsets in the northern region, especially during spring and summer, highlight the need for integrated hydrological-climatic models that incorporate snowmelt timing, groundwater processes, and land use impacts to improve drought prediction and water resource management under changing climate conditions [1]-[3] [20].

6. Conclusions

This study highlights significant spatial variability in hydrological and meteorological drought-related responses across the northern, central, and southern regions, underscoring the complex interplay between climatic drivers and water-

shed processes. The northern region exhibits the greatest temporal variability and range in break years for both baseflow and total flow, reflecting heterogeneous hydrological responses influenced by factors such as snowmelt dynamics, groundwater interactions, and land use changes. In contrast, the central and southern regions demonstrate more stable and consistent hydrological patterns, with narrower break year ranges and lower variability.

The comparison between full-period SPEI and truncated SPEI analyses reveals both important similarities and discrepancies. Both indices capture key regional and seasonal patterns in moisture availability, with the southern region consistently showing a predominance of "up" trends indicative of increased moisture or reduced drought severity, particularly during fall and summer. However, the truncated SPEI, which aligns the climatic data period with hydrological records, tends to show a higher prevalence of "no trend" categories, especially in spring and fall, suggesting relative stability in moisture conditions during these seasons. Conversely, the full SPEI dataset, spanning a longer timeframe, captures broader climatic variability and generally exhibits fewer "no trend" cases.

Despite these differences, both SPEI versions identify northern summer as a period of low agreement between climatic and hydrological trends, highlighting the complexity of hydrological responses in this region and season. The truncated SPEI provides a more temporally synchronized perspective with hydrological data, improving correspondence in certain seasons and regions, while the full SPEI offers a comprehensive view of long-term climatic variability.

Overall, these findings emphasize the necessity of considering spatial heterogeneity and temporal alignment when interpreting drought indices and their hydrological impacts. Integrating both full and truncated SPEI analyses can enhance understanding of drought dynamics and improve water resource management strategies tailored to regional and seasonal contexts under changing climate conditions.

Acknowledgements

The authors wish to thank two anonymous reviewers whose contributions greatly helped the clarity of this paper.

Conflicts of Interest

The authors declare no conflicts of interest regarding the publication of this paper. References.

References

[1] Stewart, I.T., Cayan, D.R. and Dettinger, M.D. (2005) Changes toward Earlier Streamflow Timing across Western North America. *Journal of Climate*, **18**, 1136-1155. https://doi.org/10.1175/jcli3321.1

[2] Hamlet, A.F. and Lettenmaier, D.P. (2007) Effects of 20th Century Warming and Climate Variability on Flood Risk in the Western U.S. *Water Resources Research*, **43**,

W06427. https://doi.org/10.1029/2006wr005099

[3] Dudley, R.W., Hodgkins, G.A., McHale, M.R., Kolian, M.J. and Renard, B. (2017) Trends in Snowmelt-Related Streamflow Timing in the Conterminous United States. *Journal of Hydrology*, **547**, 208-221. https://doi.org/10.1016/j.jhydrol.2017.01.051

[4] Regonda, S.K., Rajagopalan, B., Clark, M. and Pitlick, J. (2005) Seasonal Cycle Shifts in Hydroclimatology over the Western United States. *Journal of Climate*, **18**, 372-384. https://doi.org/10.1175/jcli-3272.1

[5] Slater, L. and Villarini, G. (2017) Evaluating the Drivers of Seasonal Streamflow in the U.S. Midwest. *Water*, **9**, Article 695. https://doi.org/10.3390/w9090695

[6] Byun, K., Chiu, C. and Hamlet, A.F. (2019) Effects of 21st Century Climate Change on Seasonal Flow Regimes and Hydrologic Extremes over the Midwest and Great Lakes Region of the US. *Science of the Total Environment*, **650**, 1261-1277. https://doi.org/10.1016/j.scitotenv.2018.09.063

[7] Demaria, E.M.C., *et al.* (2016) Evaluating the Drivers of Seasonal Stream Flow in US Midwest. *Journal of Climate*, **29**, 6533-6547.

[8] Schnettler, S., Sonnemann, A. and Clancy, K. (2024) Use of Groundwater, Baseflow and SPEI to Evaluate Water Resources in Michigan, USA. *Journal of Water Resource and Protection*, **16**, 640-670. https://doi.org/10.4236/jwarp.2024.1610037

[9] Steinman, A.D., Uzarski, D.G., Lusch, D.P., Miller, C., Doran, P., Zimnicki, T., *et al.* (2022) Groundwater in Crisis? Addressing Groundwater Challenges in Michigan (USA) as a Template for the Great Lakes. *Sustainability*, **14**, Article 3008. https://doi.org/10.3390/su14053008

[10] Cherkauer, K.A. and Sinha, T. (2010) Hydrologic Impacts of Projected Future Climate Change in the Lake Michigan Region. *Journal of Great Lakes Research*, **36**, 33-50. https://doi.org/10.1016/j.jglr.2009.11.012

[11] Capparelli, V., Franzke, C., Vecchio, A., Freeman, M.P., Watkins, N.W. and Carbone, V. (2013) A Spatiotemporal Analysis of U.S. Station Temperature Trends over the Last Century. *Journal of Geophysical Research*: *Atmospheres*, **118**, 7427-7434. https://doi.org/10.1002/jgrd.50551

[12] Terzi, T.B. and Önöz, B. (2024) Drought Analysis in the Seyhan River Basin Based on Standardized Drought Indices Using a New Approach Considering Seasonality. *Environmental Earth Sciences*, **84**, Article No. 30. https://doi.org/10.1007/s12665-024-12039-6

[13] Vicente-Serrano, S.M., Beguería, S. and López-Moreno, J.I. (2010) A Multiscalar Drought Index Sensitive to Global Warming: The Standardized Precipitation Evapotranspiration Index. *Journal of Climate*, **23**, 1696-1718. https://doi.org/10.1175/2009jcli2909.1

[14] Hao, Z., Singh, V.P. and Xia, Y. (2018) Seasonal Drought Prediction: Advances, Challenges, and Future Prospects. *Reviews of Geophysics*, **56**, 108-141. https://doi.org/10.1002/2016rg000549

[15] Skalbeck, J.D., Reed, D.M., Hunt, R.J. and Lambert, J.D. (2008) Relating Groundwater to Seasonal Wetlands in Southeastern Wisconsin, USA. *Hydrogeology Journal*, **17**, 215-228. https://doi.org/10.1007/s10040-008-0345-7

[16] Clancy, K.A. (2023) Standardized Baseflow Drought Index Comparison to SPEI in High Baseflow Streams. *Journal of Water Resource and Protection*, **15**, 557-580. https://doi.org/10.4236/jwarp.2023.1511031

[17] Sinha, T. and Cherkauer, K.A. (2010) Impacts of Future Climate Change on Soil Frost in the Midwestern United States. *Journal of Geophysical Research*: *Atmospheres*, **115**,

D08105. https://doi.org/10.1029/2009jd012188

[18] Burt, T.P. and Pinay, G. (2005) Linking Hydrology and Biogeochemistry in Complex Landscapes. *Progress in Physical Geography*: *Earth and Environment*, **29**, 297-316. https://doi.org/10.1191/0309133305pp450ra

[19] Tallaksen, L. and van Lanen, H. (2023) Hydrological Drought. 2nd Edition, Elsevier Science. https://www.perlego.com/book/4460002/hydrological-drought-processes-and-estimation-methods-for-streamflow-and-groundwater-pdf

[20] Sun, Y., Xu, C., Ma, M., Liu, X., Liu, L. and Yu, F. (2023) Annual, Seasonal, and Monthly Baseflow Trend in an Arid Area in Loss Plateau, China. *Water Supply*, **23**, 4855-4875. https://doi.org/10.2166/ws.2023.322

[21] USGS (US Geological Survey) (2024) Web Interface: U.S. Geological Survey National Water Information System Web Site. http://waterdata.usgs.gov/nwis/

[22] Sloto, R.A. and Crouse, M.Y. (1996) HYSEP: A Computer Program for Streamflow Hydrograph Separation and Analysis: U.S. Geological Survey Water-Resources Investigations Report 96-4040. http://pubs.er.usgs.gov/publication/wri964040

[23] Troolin, W.D. and Clancy, K. (2016) Comparison of Three Delineation Methods Using the Curve Number Method to Model Runoff. *Journal of Water Resource and Protection*, **8**, 945-964. https://doi.org/10.4236/jwarp.2016.811077

[24] World Meteorological Organization (2023) SPEI Dataset: Climatic Data and Modeling Tools.

[25] Jenson, S. (1984) Automated Derivation of Hydrological Basin Characteristics from Digital Elevation Data. US Geological Survey Report 14-08-0001-20129. http://topotools.cr.usgs.gov/pdfs/automated-derivation-of-hydrologic-basin-characteristics-from-digital-elevatioin-model-data.pdf

[26] USGS (US Geological Survey) (2019) NED (National Elevation Data) 2020 Elevation. SDE Raster Digital Data. http://nationalmap.gov/eleva

[27] Hirsch, R.M., Slack, J.R. and Smith, R.A. (1982) Techniques of Trend Analysis for Monthly Water Quality Data. *Water Resources Research*, **18**, 107-121. https://doi.org/10.1029/wr018i001p00107

[28] Hamed, K.H. and Ramachandra Rao, A. (1998) A Modified Mann-Kendall Trend Test for Autocorrelated Data. *Journal of Hydrology*, **204**, 182-196. https://doi.org/10.1016/s0022-1694(97)00125-x

[29] Jaiswal, R.K., Lohani, A.K. and Tiwari, H.L. (2015) Statistical Analysis for Change Detection and Trend Assessment in Climatological Parameters. *Environmental Processes*, **2**, 729-749. https://doi.org/10.1007/s40710-015-0105-3

[30] Mallakpour, I. and Villarini, G. (2015) A Simulation Study to Examine the Sensitivity of the Pettitt Test to Detect Abrupt Changes in Mean. *Hydrological Sciences Journal*, **61**, 245-254. https://doi.org/10.1080/02626667.2015.1008482

[31] Mendes, M.P., Rodriguez-Galiano, V. and Aragones, D. (2022) Evaluating the BFAST Method to Detect and Characterise Changing Trends in Water Time Series: A Case Study on the Impact of Droughts on the Mediterranean Climate. *Science of the Total Environment*, **846**, Article ID: 157428. https://doi.org/10.1016/j.scitotenv.2022.157428